$$t_w = -\dot{R}_o R_o/V_R^2 = 2\dot{\sigma}_o\ddot{\sigma}_o/(\ddot{\sigma}_o^2 + 4\dot{\sigma}_o^4) \quad (12)$$

It represents the time elapsing from $t_o = 0$ until actual minimum separation distance occurs between missile and target under the stated flight conditions. Unlike the time-to-go, t_g, t_w is valid for large angular deviations of the missile from the ideal collision course. From Eqs. (6, 7, and 12) it follows that t_w occurs before t_g,

$$t_w = t_g(-\dot{R}/V_R)^2 \equiv t_g \cos^2\theta_o \leqslant t_g \quad (13)$$

and in conjunction with Eq. (11)

$$t_w\dot{\sigma}_w = \ddot{\sigma}_o/2\dot{\sigma}_o^2 = 1/t_g\dot{\sigma}_o = -\cot\theta_o \quad (14)$$

Defining Equations

The necessary development has been completed for the prediction of LOS angle, rate, and acceleration as well as range and range rate at the instant of closest separation.

Integration of Eq. (10) with initial conditions gives the range $R(t)$ in the form

$$R^2 = R_o^2\dot{\sigma}_o[1 + \dot{\sigma}_w^2(t_w - t)^2]/\dot{\sigma}_w \quad (15)$$

Identification with Eq. (8) leads to the expression for LOS angular rate $\dot{\sigma}$,

$$\dot{\sigma}(t) = \dot{\sigma}_w/[1 + \dot{\sigma}_w^2(t_w - t)^2] \quad (16)$$

which reduces at time $t = t_w$ to $\dot{\sigma}(t_w) \equiv \dot{\sigma}_w$. Hence, Eq. (11) represents the LOS rate at t_w as predicted from the initial values at the instant of observation.

Integration of Eq. (16) with initial conditions provides a prediction expression for the LOS angle $\sigma(t)$ in the implicit form

$$\tan[\sigma(t) - \sigma_o] = \dot{\sigma}_w t/[1 + \dot{\sigma}_w^2 t_w(t_w - t)] \quad (17)$$

Differentiation of Eq. (16) leads to the desired expression for LOS angular acceleration $\ddot{\sigma}$,

$$\ddot{\sigma}(t) = 2\dot{\sigma}_w^3(t_w - t)/[1 + \dot{\sigma}_w^2(t_w - t)^2]^2 \quad (18)$$

With the aid of Eq. (16), it can be written in a useful alternate form

$$(t_w - t)\dot{\sigma}_w = \ddot{\sigma}/2\dot{\sigma}^2 \quad (19)$$

which when evaluated at $t_o = 0$ gives the interesting relation $\dot{\sigma}_w t_w\dot{\sigma}_o t_g = 1$ in agreement with Eq. (14).

The LOS acceleration $\ddot{\sigma}(t)$, as defined by Eq. (18) has a maximum and minimum (in that order, if $\dot{\sigma}_o > 0$) located symmetrically about the zero at $t = t_w$. It also possesses three inflection points, one of which is the time t_w of closest approach. By conventional successive differentiation and equating the results to zero, these critical times are found to be

$$\text{extremes:} \qquad t_e = t_w \pm 1/3^{1/2}\dot{\sigma}_w \quad (20)$$

$$\text{inflections:} \qquad t_i = t_w, \quad t_i = t_w \pm 1/\dot{\sigma}_w \quad (21)$$

The time t_e will provide the value of the first extreme of $\ddot{\sigma}$ (occurring before closest separation is reached), which is of importance in estimating the saturation constraint in the gimbal design of tracking systems.[3]

Predicted Terminal Values

Evaluation of the expressions for kinematic variables previously developed at the time t_w, of closest separation is straightforward using Eq. (12) in the case of the three passive variables (LOS angle, rate, and acceleration). Table 1 summarizes the quantity, its name, defining equation number, and evaluated expression at various times of interest, as well as t_w. Figure 2 identifies those times in the over all behavior of the kinematic variables. (Reference 4 develops curves similar to those of Fig. 2, normalized as a function of nondimensionalized time, for the case of a ground fixed radar site tracking a crossing target whose course and speed are specifiable a priori).

Evaluation of the range $R(t)$ at the time t_w predicts the exact miss distance[2]

$$R_w = 2R_o\dot{\sigma}_o^2/(\ddot{\sigma}_o^2 + 4\dot{\sigma}_o^4)^{1/2} = R_o^2|\dot{\sigma}_o|/V_R \quad (22)$$

as a function of initial observations. Note an initial range measurement R_o is required for the prediction. The linearized approximation to miss distance is predicted at time-to-go t_g, and is given[2] by

$$R_w \cong M_g = R_o|\dot{\sigma}_o|t_g \quad (23)$$

Both these miss distances are shown in Fig. 1 and 2.

The usual linearization process provides the approximations for range rate as $\dot{R}_o \cong -V_R$, a constant, and range as $R \cong -\dot{R}_o(t_g - t)$. For comparison with the exact expressions, rewrite Eq. (10) for range rate in the form

$$\dot{R}(t) = -V_R|\dot{\sigma}_w|(t_w - t)[1 + \dot{\sigma}_w^2(t_w - t)^2]^{-1/2} \quad (24)$$

and Eq. (15) for range as

$$R(t) = V_R(t_w - t)[1 + \dot{\sigma}_w^{-2}(t_w - t)^{-2}]^{1/2} \quad (25)$$

These functions, together with their linearized approximations are also shown as functions of time in Fig. 2. Note the approximation $\dot{R}_o$ for $\dot{R}$ exhibits the wrong sign before t_g is attained (after t_w has already occurred).

References

[1] Rawling, A. G., "Passive Determination of Homing Time," *AIAA Journal*, Vol. 6, No. 8, Aug. 1968, pp. 1604–1606.

[2] Rawling, A. G., "On Non-Zero Miss Distance," *Journal of Spacecraft and Rockets*, Vol. 6, No. 1, Jan. 1969, pp. 81–83.

[3] Gebhart, C., "Intercept Dynamics," *National Aerospace Electronics 1963 Proceedings*, Dayton Section Professional Group on Aerospace and Navigation Electronics, Dayton, Ohio, pp. 46–53.

[4] Chestnut, H. and Mayer, R. W., *Servomechanisms and Regulating System Design*, 1st ed., Vol. 2, Wiley, New York, 1955, pp. 44–49.

Lumped-Parameter Modeling vs Distributed-Parameter Modeling for Fluid Control Lines

G. M. SWISHER*
Wright State University, Dayton, Ohio

AND

E. O. DOEBELIN†
Ohio State University, Colombus, Ohio

THE over-all performance of a hydraulic control system is determined in part by the dynamic characteristics of the transmission lines connecting the components of the systems. Failure to account for transmission line dynamics can lead to serious errors in system design. Ezekiel and Paynter[1] derived ordinary differential equations in hyperbolic operators relating pressures and flows at two cross sections of a hydraulic line. These equations were referred to as the water-hammer equations or transfer function of the fluid lines. The literature abounds with line-dynamics information, but no investigator has applied this knowledge to the study of the interactions of line dynamics with complete control systems.

Received February 25, 1970.

* Assistant Professor of Engineering.

† Professor of Mechanical Engineering.

The system studied was a closed-loop electro-hydraulic position servo consisting of 1) a hydraulic cylinder as the power device, 2) two linear variable differential transformers (LVDT's) as the feedback and measurement elements, 3) an electronic servo-amplifier with a summing circuit for comparing voltages representing the actual and desired positions of the cylinder, 4) a servovalve driven by an electromagnetic torque motor, 5) hydraulic lines connecting the ports of the cylinder with the ports of the servovalve, 6) a full-wave-phase sensitive demodulator which receives the measurement LVDT signal, and 7) a frequency response analyzer which provides the sinusoidal test signal and analyzes the return signal to give frequency response data.

Comparisons were made between three models of the fluid lines and the experimental results. The dynamic response was defined as the actual position of the piston versus the desired position of the piston. The simplest line model is obtained by assuming that the pressures and flows remain uniform all along the line. This neglects fluid inertia and friction. The effect of fluid compressibility in the line is accounted for by including the volume of fluid in the line with the piston enclosed volume. This is referred to as the no-inertia line model.

Another assumption in common use today is that the fluid line can be represented by several "lumps." Each lump may have compliance, friction, and inertia as desired. The number of lumps necessary for results that compare favorably with the distributed parameter results is a reasonable question to ask. Experience has shown that a good rule of thumb is to select the number of lumps such that there are ten lumps per wavelength at the highest frequency of interest. Here it is necessary to have some estimate of the frequency spectrum of the expected input signals. "Wavelength" λ refers to the wavelength of signal propagation in a continuous fluid medium and is governed by the usual law for systems governed by the wave equation, namely

$$\lambda \triangleq \text{velocity of propagation/frequency} \tag{1}$$

The pressures and velocities are assumed to be uniform for each lump of fluid. Newton's law for a lump of fluid gives:

$$P_{n-1} - P_n = \rho_0 a s V_n \tag{2}$$

where P_{n-1} and P_n are Laplace transforms of pressure at lumps $n-1$ and n, respectively; ρ_0 is the mass density of the fluid, a is the lump length, s is the Laplace variable, and V_n is the Laplace transform of velocity of lump n.

For a short time dt, conservation of mass for the nth lump gives:

$$v_{n-1} - V_n = a K_c s P_n \tag{3}$$

where K_c is the combined line and fluid compliance. These two equations give the desired number of equations for the number of lumps necessary to have 10 lumps per wavelength.

The third type of analysis considers the distributed-parameter nature of the fluid lines. The equations obtained here, in general, are the water-hammer partial differential equations. They are derived in Ref. 2 and are shown here in the Laplace transformed state:

$$\cosh\beta_1 P(0,s) - z_0 \sinh\beta_1 V(0,s) = P(L,s) \tag{4}$$

$$-1/z_0 \sinh\beta_1 P(0,s) + \cosh\beta_1 V(0,s) = V(L,s) \tag{5}$$

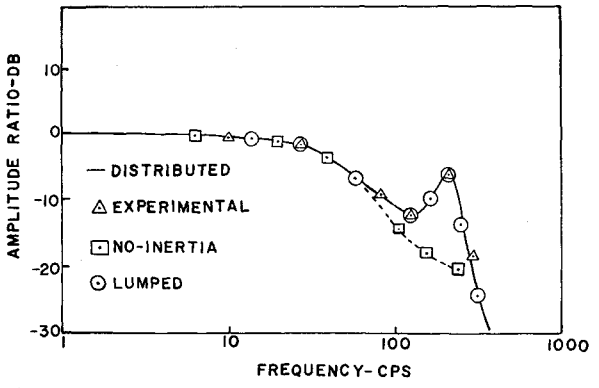

Fig. 1 Frequency responses of output piston motion vs desired piston motion for various fluid line models.

where $P(0,s)$ and $V(0,s)$ are Laplace transforms of pressure and velocity, respectively, at any station; $P(L,s)$ and $V(L,s)$ are Laplace transforms of pressure and velocity at distance L down the line; z_0 is the characteristic hydraulic impedance of line; and β_1 is the characteristic function of Laplace variable, s.

All three types of analyses lead to tedious algebra in order to obtain the frequency response between the output piston motion and the input voltage. In the case of the no-inertia model there were 5 simultaneous equations. The 10 lump per wavelength model required 13 equations and the distributed parameter model required 9 equations. The procedure adopted was the numerical solution by a IBM-360 digital computer at each frequency.

Facts of interest with respect to the experimental test might be listed as follows: 1) input sine wave frequency was limited to the range of 1 cps to 1000 cps; 2) input sine wave amplitude was 4.0 v peak to peak (this corresponded to a piston motion of 0.020 in. peak to peak).

The comparison of the three models and the experimental results is shown in Fig. 1. Only the amplitude ratio is shown for the transfer function relating the input voltage to the output piston position. The distributed-parameter and the 10 lump per wavelength models agree very well with the experimental results for all frequencies. The validity of no-inertia breaks down at about 90 cps. The lumped model is recommended for design purposes when a digital computer is not available to the hydraulic designer or when the number of lumps is 2 or less. With increasing number of lumps the complex algebra involved in solving for the frequency response nullifies the advantage of simplicity that the lumped-parameter model has. In addition, the author noted that the 10 lump per wavelength model took 4 times more computer time than the distributed parameter model when a matrix inversion technique was used to solve for the frequency responses.

References

[1] Ezekiel, F. D. and Paynter, H. M., "Fluid Power Transmission," *Fluid Power Control*, 1st ed., Technology Press of M.I.T. and Wiley, New York, 1960, pp. 130–140.

[2] Swisher, G. M., "A Theoretical and Experimental Investigation of the Dynamics of Hydraulic Control Systems Connected by Long Lines or Hoses," Ph.D. dissertation, 1969, The Ohio State Univ., Columbus, Ohio.